Progress In Electromagnetics Research Letters, Vol. 100, 91–97, 2021

Terahertz Off-Axis Focus Polarization Converter Based on Metasurface

Bo Yin[1, 2], Zhu Xu[1, *], and Yue Ma[1]

Abstract—In order to satisfy the requirements of terahertz time-domain spectrum system under specific circumstances, an off-axis focus reflective polarization converter in terahertz band is proposed. By combining the principle of phase compensation and phase gradient metasurface, a reflective array containing 20×20 units is designed. The phase distribution along the metasurface is calculated through the principle of optical path reversibility. Geometric rotation and resonant frequency modulation constitute the phase change of the unit that can overlap one another without interference. Compared with the conventional reflective polarization converter in terahertz band, the proposed one could reflect the normally incident terahertz wave while providing larger energy at the focus. The simulation results show that the proposed polarization converter has good performance in both polarization conversion and electromagnetic focus, which has significant practical application in numerous situations.

1. INTRODUCTION

In recent years, since metasurface reveals its irreplaceable properties including negative dielectric constant and negative magnetic permeability [1, 2], numerous researches and designs have been proposed based on metasurfaces [3, 4]. Because of their designable equivalent electromagnetic parameters, metasurfaces offer researchers great freedom in modulating electromagnetic wave fronts by varying the shape [5], size [6], and material of tiny structures [7, 8]. The polarization converter devices based on metasurface are characterized by the metasurface's thickness, small physical size, and high integration [9, 10], can even be tunable [11], and provide a new solution to the size of conventional polarization converters while meet the application requirements of terahertz systems [12, 13].

Conventional polarization converter based on metasurface is composed of periodically placed unit cells [14–17], and its propagation follows the Snell's law. The polarization conversion ratio (PCR) of conventional reflective polarization convertors based on metasurface would sharply decrease with the increase of the incident angle, so its potential application prospects are limited [18, 19]. In [20], Yu et al. explained the Generalized Snell's Law by introducing phase discontinues along the surface. In addition, they have proposed a structure containing eight different V-shaped structures which offer different reflecting phases. The proposed metasurface which is called phase gradient metasurface (PGM) could reflect the normally incident electromagnetic (EM) wave to a specific angle. According to this theory, anomalous reflective polarization converter can be realized. In [21], a polarization converter with high-efficiency PCR based on PGM consisting of 6 units with different arc lengths is proposed. The measurement results of anomalous reflecting angle are in good agreement with the theoretical ones. In [22], Zhuang et al. proposed a reflective linear-circular polarization converter based on PGM. In the frequency range of 13.5–15.4 GHz, linearly polarized (LP) wave can be converted into circularly

Received 18 July 2021, Accepted 1 September 2021, Scheduled 1 October 2021

* Corresponding author: Zhu Xu (1826113722@qq.com).

[1] School of Optoelectronic Engineering, Chongqing University of Posts and Telecommunications, Chongqing 400065, China.

[2] Chongqing Municipal Level Key Laboratory of Photoelectronic Information Sensing and transmitting Technology, Chongqing, 400065, China.

polarized (CP) wave, and the axial ratio is less than 3 dB. Considering the poor linearity of cross-polarized reflecting phase, the performance of anomalous reflection is degraded, although the PCR of each unit is high. In [23], a novel design of reflective linear and multifunctional polarization converter is proposed. Broadband and simultaneous linear and circular polarization conversion can be realized by changing the super surface volume. In [24], a broadband polarization converter with anomalous reflection in terahertz band is proposed. From 0.40 to 0.60 THz, the variation range of reflection angle is 39° to 20°, and the side lobe level is less than −14 dB. This expands the application of polarization converter in terahertz band.

Under certain circumstances, such as in terahertz communication system or other situations which need concentrate the energy of polarization converter, conventional polarization converter suffers penalties in integration because the researchers usually need to attach an additional flat lens to it. To address this problem while improving the reflection efficiency, an off-axis focused terahertz polarization converter based on a phase compensation mechanism is proposed. Consisting of different H-shaped unit cells, this design has a focal length of 30.0 mm and off-axis 4.0 mm. The phase of each unit has changed because of the geometric rotation and resonant frequency modulation, which can be superimposed on each other without interference [25]. The E-field distribution along different planes shows that the proposed polarization converter has both good focusing and polarization conversion ability.

2. THEORY

To concentrate the reflected EM wave to a specific spot $F_0(x_0, y_0, z_0)$, the reflecting E-filed along the metasurface should be [26]:

$$E_r = A_0\left(x_i, y_j\right) \exp\left(j\varphi_0\left(x_i, y_j\right)\right) \tag{1}$$

where (x_i, y_j) refers to the unit cell in the coordinate of the center of the metasurface of the ith row and jth column. $A_0(x_i, y_j)$ and $\varphi_0 = (x_i, y_j)$ refer to the amplitude and phase of the unit cell, respectively. In order to achieve good overall PCR, the reflectance of each unit cell should be high. The phase distribution should be:

$$\varphi_0\left(x_i, y_i\right) = D_0 \exp\left(-jk_0\left|F_0 - r_i\right|\right) \tag{2}$$

where D_0 refers to the E-filed amplitude at F_0, and k_0 is the free space wave number. In this design, the incident wave is normally incident along the z-axis. Thus, Eq. (2) can be changed to:

$$\varphi_0\left(x_i, y_i\right) = -k_0 d_i + \varphi_i\left(x_i, y_i\right) \tag{3}$$

where d_i refers to the distance between unit cell and focus, and $-k_0 d_i$ is the phase when the planewave reaches the metasurface. The phase center of the planewave is $(0, 0, z_f)$. The reflecting phase of the unit cell is:

$$\varphi_i = k_0\left(\left|-x_i, -y_i, z_f\right| + \left|x_0 - x_i, y_0 - y_i, z_0\right|\right) \tag{4}$$

3. DESIGN AND DISCUSSION

According to the theory of the phase compensation mechanism, the cross-reflecting phase of each unit in the metasurface can be obtained. The focal length of the design is 30.0 mm. The period of each unit is $P = 200.0$ um. The metasurface contains 20×20 units. Fig. 1 shows the schematic of the proposed polarization converter. Based on the theory in Section 2, the reflecting phase distribution of cross-polarization is calculated through MATLAB when the focal length is set to 30 mm, which is about fifty times of wavelength at 0.5 THz. The phase distribution along the metasurface is displayed in Fig. 2.

According to Fig. 2, the requirement of the phase coverage is 0–360°. In addition, the phase difference between adjacent units is small. Fig. 3 and Fig. 4 display that the reflective polarization converter device based on PGM has three layers, including an upper metallic pattern layer, an intermediate dielectric layer, and a metallic ground reflector. Gold with a thickness of 0.20 μm is selected as the upper metallic pattern layer. The material of the intermediate dielectric layer is polyamide substrate, the dielectric function of $\varepsilon = 3.5$ with a thickness of 75.00 μm. A gold plate with a thickness of 0.20 μm is placed under the polyamide substrate as the ground reflector. A sticking layer of titanium

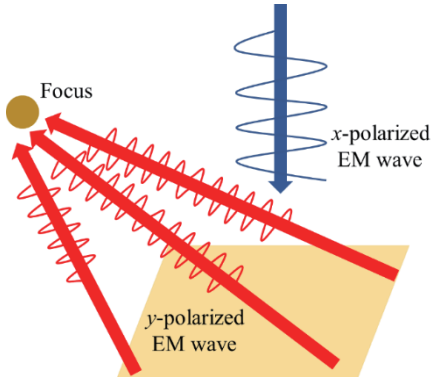

Figure 1. The schematic of off-axis focus polarization conversion.

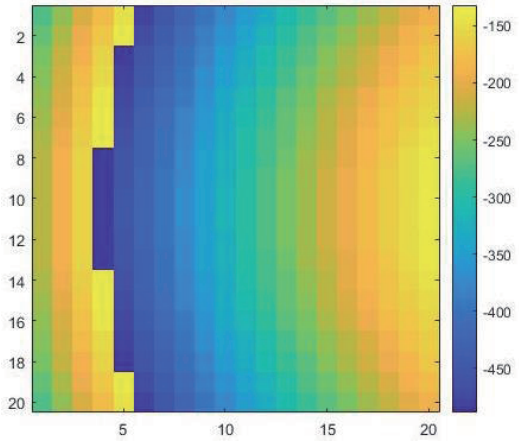

Figure 2. The reflecting phase distribution of cross-polarization.

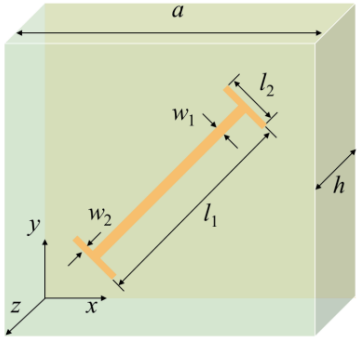

Figure 3. The schematic of single unit.

Figure 4. The side view of the unit.

with a thickness of 0.05 μm is used as the middle layer of the gold layer and substrate because of the poor adhesion between the polyamide and gold.

The phase coverage could be divided into two parts: the geometric phase modulation through rotating the metal pattern and the resonate frequency shift phase modulation. To achieve perfect reflecting phase distribution, it is necessary to analyze the reflecting phase of cross-polarization in terms of varied parameters. By adding two resonant branches at both ends of the cut-wire structure, the broadband high PCR is realized. This branch length could adjust the path length of the surface current, which could alter the resonating frequency and reflecting phase of the unit.

Figure 5 illustrates the reflecting phase of cross-polarization and PCR according to different branch lengths l_2. As the branch length increases from 60 μm to 90 μm with a step width of 10 μm, the PCR in the lower band decreases, which is because the branch length mainly tunes the resonating frequency of the lower band. Though the operating bandwidth increases, the PCR at 0.5 THz deteriorates dramatically. On the other hand, the cross-polarized reflecting phase at 0.5 THz decreases 7 to 9° as the branch increases 10 μm.

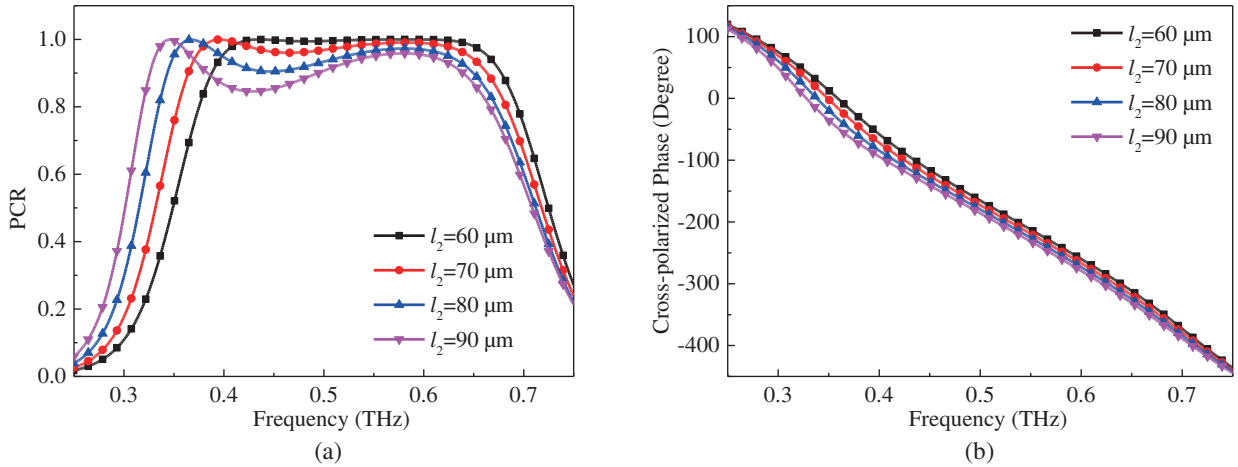

Figure 5. The performance in terms of varying resonant branch length. (a) PCR in terms of varying resonant branch length. (b) Reflecting phase of cross-polarization in terms of different resonant branch length.

According to these results, the impact on PCR from varying resonant branches is relatively large. Considering that a minor tolerance may cause a relatively large shifting in PCR, another parameter should be attached in order to achieve good modulation.

Figure 6 illustrates the reflecting phase of cross-polarization and PCR according to different cut-wire lengths l_1. By changing the cut-wire length, the resonating frequency and surface current path could also be changed. According to Fig. 5, with the same step width of resonant branch length of 10 μm, the variation of cross-polarized reflecting phase is larger than the former ones. The decrease is about 8 to 12° which means that subtle adjustments of cross-polarized reflecting phase can be achieved through changing branch length l_2. The PCR in the lower band decreases as the cut-wire length increases, causing the bandwidth narrowing. However, the PCR at 0.5 THz just has some minor changes. By combining the variation of both branch length and cut-wire length, the cross-reflecting phase distribution can be achieved while maintaining high PCR.

Figure 7 displays the schematic of the off-axis focus polarization converter array. The unit arrangement is mirror symmetric. All units match the phase distribution calculated by MATLAB with errors less than 1°. In addition, the PCR of each unit is higher than 0.85 at 0.5 THz. In CST studio suite, the proposed polarization convert array is simulated. And the boundary conditions along x-, y-, and z-directions are open and add space. The E-filed distributions along different planes with x-polarized EM wave normally incident are illustrated in Fig. 8. According to the xoz cross-section of the E-filed in y-direction, the distribution of the E-filed in space has a relatively obvious clustering

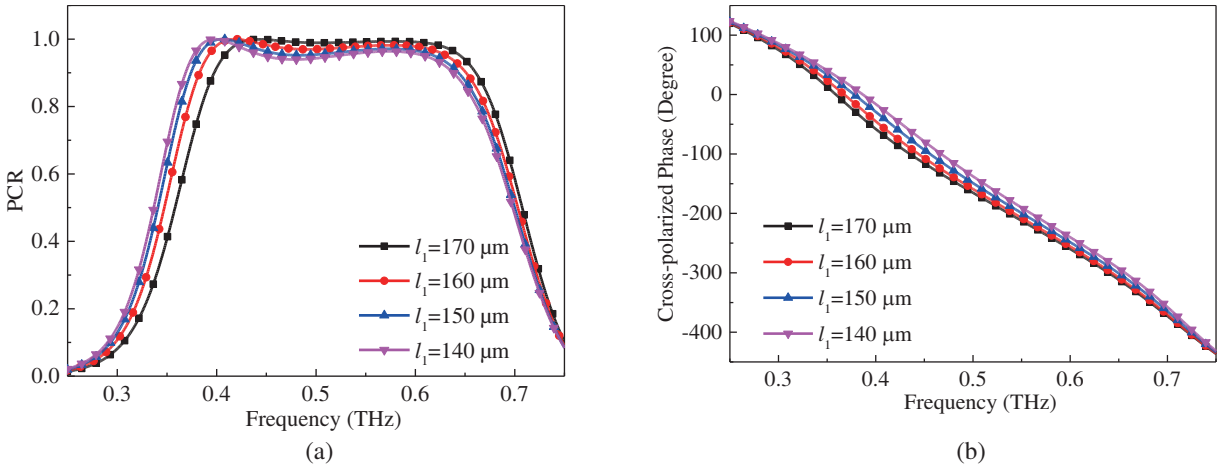

Figure 6. The performance in terms of varying cut-wire length. (a) PCR in terms of varying cut-wire length. (b) Reflecting phase of cross-polarization in terms of different cut-wire length.

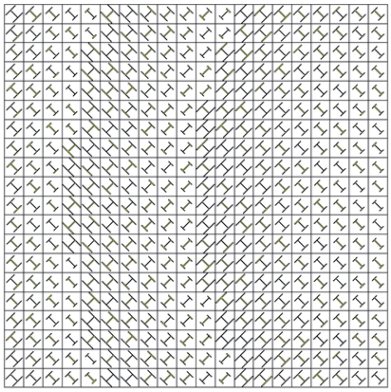

Figure 7. The schematic of off-axis focus polarization converter array.

effect. The E-filed in the red circle is obviously larger than the nearby electric field, indicating a certain focusing effect. In addition, the E-filed in the red circle is about 1.6 V/m, which is larger than the incident EM wave of 1 V/m, indicating that the energy has been focused at this position. However, the focal position is at a distance from the metasurface about 25 mm, which is slightly different from the original 30 mm. This may be because the cross-polarized reflecting phase of each different unit is calculated under periodic boundary setting. In actual array, adjacent units are not the same, which may result in electromagnetic couple, causing the reflecting phase of cross-polarization changing.

It can be observed that there is still E-filed along the x-direction on the xoz plane. This is because the incident field and reflecting field cannot be separated by CST studio suite under time domain simulation. The E-filed along the x-direction on xoz plane is distributed in the vertical direction, indicating that the E-fileds in these x-directions are incident fields. According to the E-filed distribution along the y-direction on the yoz plane, the focusing effect is very obvious. However, it can be found that it has a long depth of focus which may be caused by a relatively small metasurface array. The E-filed distribution in the x-direction on this cross-section is the same as the xoz cross-section, which is uniformly perpendicular. This can also indicate that these electric fields in the x-direction are the electric fields of incident electromagnetic waves. The electric field distribution in the y-direction on the xoy cross-section can be found to have obvious focal spots, and the electric field at the centre of the focal spot is about 1.7 V/m. In summary, although the focusing position has some errors with the design requirements, this off-axis focusing polarization converter array still has good focusing effect.

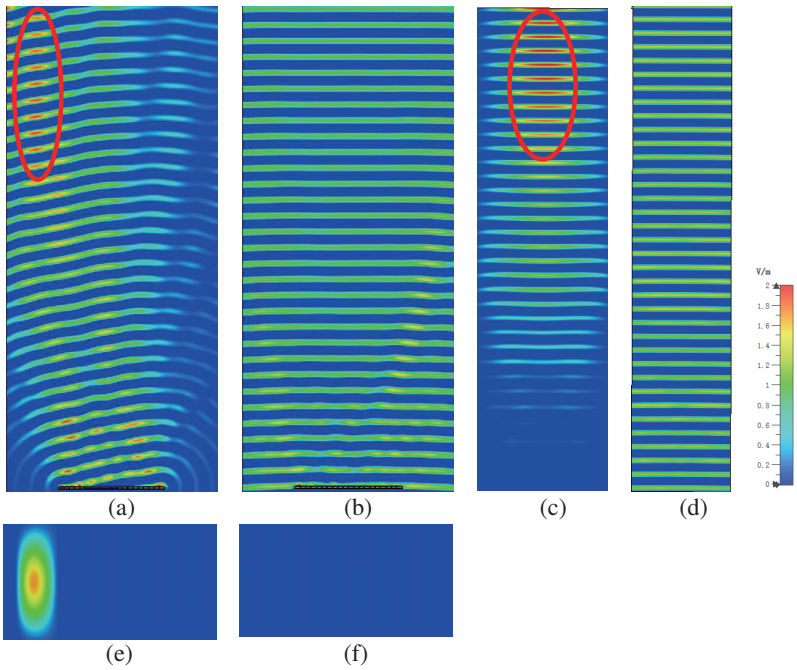

Figure 8. The E-filed distribution along different planes at 0.50 THz. (a) E-filed on y-direction on xoz plane. (b) E-filed on x-direction on xoz plane. (c) E-filed on y-direction onyoz plane. (d) E-filed on x-direction on yoz plane. (e) E-filed on y-direction on xoy plane. (f) E-filed on x-direction on xoy plane.

4. CONCLUSION

In this paper, a terahertz off-axis focus polarization converter based on PGM is proposed. By adjusting the resonating frequency of the polarization convert unit, a set of units which could satisfy the phase distribution while maintain high PCR is designed. It can be seen from the E-filed distribution along different planes that the proposed metasurface array could convert the LP EM wave to its cross polarization when focusing at 25 mm away from the metasurface. The results show that the proposed polarization converter has good PCR and focus performance, which provides potentials in many applications such as time-domain spectrum and terahertz communication system.

ACKNOWLEDGMENT

This work was supported by the National Natural Science Foundation of China (NO. 61871063) and Chongqing Technology Innovation and Application Development Project (cstc2019jscx-msxmX0079).

REFERENCES

1. Ling, F., et al., "A broadband tunable terahertz negative refractive index metamaterial," *Scientific Reports*, Vol. 8, No. 1, 1–9, 2018.
2. Suzuki, T., et al., "Negative refractive index metamaterial with high transmission, low reflection, and low loss in the terahertz waveband," *Optics Express*, Vol. 26, No. 7, 8314–8324, 2018.
3. Luo, H. and Y. Cheng, "Dual-band terahertz perfect metasurface absorber based on bi-layered all-dielectric resonator structure," *Optical Materials*, Vol. 96, 109279, 2019.
4. Tian, Y., et al., "High transmission focusing lenses based on ultrathin all-dielectric Huygens' metasurfaces," *Optical Materials*, Vol. 109, 110358, 2020.
5. Katrodiya, D., et al., "Metasurface based broadband solar absorber," *Optical Materials*, Vol. 89, 34–41, 2019.

6. Khan, A. D., et al., "Light absorption enhancement in tri-layered composite metasurface absorber for solar cell applications," *Optical Materials*, Vol. 84, 195–198, 2018.
7. Bashirpour, M., et al., "Terahertz radiation enhancement in dipole photoconductive antenna on LT-GaAs using a gold plasmonic nanodisk array," *Optics & Laser Technology*, Vol. 120, 105726, 2019.
8. Li, J., et al., "Addressable metasurfaces for dynamic holography and optical information encryption," *Science Advances*, Vol. 4, No. 6, eaar6768, 2018.
9. Grady, N. K., et al., "Terahertz metamaterials for linear polarization conversion and anomalous refraction," *Science*, Vol. 340, No. 6138, 1304–1307, 2013.
10. Chen, X., et al., "High-efficiency compact circularly polarized microstrip antenna with wide beamwidth for airborne communication," *IEEE Antennas and Wireless Propagation Letters*, Vol. 15, 1518–1521, 2016.
11. Xu, K.-D., et al., "Tunable multi-band terahertz absorber using a single-layer square graphene ring structure with T-shaped graphene strips," *Optics Express*, Vol. 28, No. 8, 2020, doi:10.1364/OE.390835.
12. Wen, D., et al., "Metasurface for characterization of the polarization state of light," *Optics Express*, Vol. 23, No. 8, 10272–10281, 2015.
13. Zheng, Q., et al., "Wideband, wide-angle coding phase gradient metasurfaces based on Pancharatnam-Berry phase," *Scientific Reports*, Vol. 7, No. 1, 1–13, 2017.
14. Xu, J., et al., "Ultra-broadband linear polarization converter based on anisotropic metasurface," *Optics Express*, Vol. 26, No. 20, 26235–26241, 2018.
15. Luo, F., et al., "Multiband terahertz reflective polarizer based on asymmetric L-shaped split-ring-resonators metasurface," *2016 11th International Symposium on Antennas, Propagation and EM Theory, ISAPE). IEEE*, 2016.
16. Zou, M., M. Su, and H. Yu, "Ultra-broadband and wide-angle terahertz polarization converter based on symmetrical anchor-shaped metamaterial," *Optical Materials*, Vol. 107, 110062, 2020.
17. Gandhi, C., P. R. Babu, and K. Senthilnathan, "Designing abroadband terahertz half-wave plate using an anisotropic metasurface," *Journal of Infrared, Millimeter, and Terahertz Waves*, Vol. 40, No. 5, 500–515, 2019.
18. Cao, H., et al., "Dual-band polarization angle independent 90 polarization rotator using chiral metamaterial," *IEICE Electronics Express*, Vol. 13, No. 15, 20160583–20160583, 2016.
19. Wang, Z., et al., "Huygens metasurface holograms with the modulation of focal energy distribution," *Advanced Optical Materials*, Vol. 6, No. 12, 1800121, 2018.
20. Yu, N., et al., "Light propagation with phase discontinuities: generalized laws of reflection and refraction," *science*, Vol. 334, No. 6054, 333–337, 2011.
21. Yu, J.-B., et al., "High-efficiency ultra-wideband polarization conversion metasurfaces based on split elliptical ring resonators," *Acta PhysicaSinica*, Vol. 64, No. 17, 2015.
22. Zhuang, Y.-Q., et al., "Design of reflective linear-circular polarization converter based on phase gradient metasurface," *Acta PhysicaSinica*, Vol. 65, No. 15, 2016.
23. Chakravarty, S. and D. Mitra, "A Novel Ultra-Wideband and Multifunctional Reflective Polarization Converter," *2020 IEEE 17th India Council International Conference, INDICON). IEEE*, 2020.
24. Yin, B. and M. Yue, "Broadband terahertz polarization converter with anomalous reflection based on phase gradient metasurface," *Optics Communications*, Prepublish, 2021, doi: 10.1016/J.OPTCOM.2021.126996.
25. Shi, H., et al., "Gradient metasurface with both polarization-controlled directional surface wave coupling and anomalous reflection," *IEEE Antennas and Wireless Propagation Letters*, Vol. 14, 104–107, 2014.
26. Zhang, P., et al., "Design, measurement and analysis of near-field focusing reflective metasurface for dual-polarization and multi-focus wireless power transfer," *IEEE Access*, Vol. 7, 110387–110399, 2019.